Published in final edited form as:
Histochem Cell Biol. 2012 August ; 138(2): 201–213. doi:10.1007/s00418-012-0959-7.

Plasmid DNA is internalized from the apical plasma membrane of the salivary gland epithelium in live animals

Monika Sramkova, **Andrius Masedunskas**, and **Roberto Weigert***
Intracellular Membrane Trafficking Unit, Oral and Pharyngeal Cancer Branch, National Institute of Dental and Craniofacial Research, National Institutes of Health, 30 Convent Drive Room 303, Bethesda, MD 20892-4340, USA

Abstract

Non viral-mediated gene delivery represents an alternative way to express the gene of interest without inducing immune responses or other adverse effects. Understanding the mechanisms by which plasmid DNAs are delivered to the proper target *in vivo* is a fundamental issue that needs to be addressed in order to design more effective strategies for gene therapy. As a model system, we have used the submandibular salivary glands in live rats and we have recently shown that reporter transgenes can be expressed in different cell populations of the glandular epithelium, depending on the modality of administration of plasmid DNA. Here, by using a combination of immunofluorescence and intravital microscopy, we have explored the relationship between the pattern of transgenes expression and the internalization of plasmid DNA. We found that plasmid DNA is internalized: 1) by all the cells in the salivary gland epithelium, when administered alone 2) by large ducts, when mixed with empty adenoviral particles, and 3) by acinar cells upon stimulation of compensatory endocytosis. Moreover, we showed that plasmid DNA utilizes different routes of internalization, and evades both the lysosomal degradative pathway and the retrograde pathway towards the Golgi apparatus. This study clearly shows that *in vivo* approaches have the potential to address fundamental questions on the cellular mechanisms regulating gene delivery.

Keywords

Intravital microscopy; plasmid DNA; endocytosis; salivary glands; gene therapy; non-viral gene delivery

Introduction

The ability to express genes in live organisms is a formidable tool that is used both for basic research and clinical applications (i.e. gene therapy). Two main strategies have been adopted to deliver and express the gene of interest: one based on viral vectors, and the other based on non viral-mediated approaches (Anwer et al., 2000; Kawakami, 2008; Kay, 2011; Lavigne and Gorecki, 2006). Viral-based gene transfer is very effective and leads to high yields of transgene expression (Young et al., 2006). Several viruses have been used for these purposes and novel strains are continuously investigated for their use *in vitro*, in animal models and in clinical trials (Bouard et al., 2009; Walther and Stein, 2000). Non viral-based methods, although limited by low levels of expression, are preferable for gene therapy since they do not induce any significant adverse effects, such as immune responses or unwanted infections(Al-Dosari and Gao, 2009). The use of plasmid or “naked” DNA for gene delivery

*To whom the correspondence should be addressed: weigertr@mail.nih.gov.

has increased since the first demonstration of *in vivo* gene transfer by intramuscular injection in live rodents (Wolff et al., 1990). Up to 2007, almost 30 % all of gene therapy clinical trials use naked DNA (Edelstein et al., 2007). In order to increase the efficiency of transgene expression the use of plasmid DNA has been combined with different methods such as hydrodynamic delivery, electroporation, gene gun transfer, ultrasounds or use of DNA complexes with cationic polymers and lipids (Kawakami, 2008; Passineau et al., 2010). However, to further improve the yields of expression and design better and more effective strategies, it is fundamental to fully elucidate the mechanisms by which plasmid DNA is internalized by cells, and traffic intracellularly. Several observations indicate that endocytosis is one of the main routes utilized for plasmid DNA uptake (Al-Dosari and Gao, 2009; Lechardeur and Lukacs, 2002). Distinct endocytic pathways have been implicated in DNA uptake, such as phagocytosis, pinocytosis, receptor-mediated endocytosis, and internalization mediated by caveolae (Budker et al., 2000; Khalil et al., 2006; Schnitzer et al., 1994; Wolff et al., 1992). After the internalization, plasmid DNA has been proposed to escape the endosomal system by mechanisms that are not yet completely understood and that may involve the osmotic rupture of the endosomal membrane (Khalil et al., 2006; Medina-Kauwe et al., 2005). This strategy permits the plasmid DNA to reach the cytoplasm, thus avoiding its delivery to the lysosomes and its consequent degradation (Varkouhi et al., 2011). Finally, plasmid DNA can access the transcription machinery either via import into the nucleus or after the nuclear envelope breakdown that occurs during mitosis (Khalil et al., 2006; Medina-Kauwe et al., 2005; Varkouhi et al., 2011).

Most of the studies on DNA uptake and trafficking have been performed in cultured cells that provide a powerful experimental system to study these processes. However, the mechanisms of gene delivery have recently began to be investigated in fully developed tissues in live animals (Fumoto et al., 2009; Wolff and Budker, 2005). In this respect, salivary glands are one of the most promising experimental models for this kind of studies. First, the epithelium of these organs can be easily accessed from the oral cavity in a non-invasive fashion, by introducing fine polyethylene tubing into the major excretory ducts (Wharton's duct in the submandibular glands and Stensen's duct in the parotid glands). This route, that has been utilized to selectively deliver various molecules into the ductal system, has been extensively characterized for both viral- and non viral-mediated gene transfer both in animals and in humans (Adriaansen et al., 2008; Adriaansen et al., 2011; Adriaansen et al., 2010; Baccaglini et al., 2001; Baum et al., 2006; Delporte et al., 1997; Gao et al., 2011; Goldfine et al., 1997; Honigman et al., 2001; Niedzinski et al., 2003a; Niedzinski et al., 2003b; Perez et al., 2011; Samuni et al., 2008; Xu et al., 2010; Zheng and Baum, 2011; Zheng and Baum, 2005; Zheng et al., 2011a; Zheng et al., 2006; Zheng et al., 2011b; Zheng et al., 2011c). Second, we have shown that salivary glands are ideal organs to perform intravital microscopy, which enables imaging various biological processes in live animals (Masedunskas et al., 2012; Masedunskas et al., 2011; Masedunskas and Weigert, 2008; Sramkova et al., 2009; Weigert et al., 2010). Specifically, we have shown that membrane trafficking events, such as endocytosis and exocytosis, can be studied in real time in the salivary glands of live rodents (Masedunskas et al., 2012; Masedunskas et al., 2011; Masedunskas and Weigert, 2008). Moreover, we have recently described how the pattern of expression of fluorescently labeled reporter molecules expressed in the submandibular glands of live rats is modulated by administering plasmid DNA under different experimental conditions (Sramkova et al., 2009).

Here we used a combination of intravital microscopy and immunofluorescence to follow the fate of plasmid DNA upon administration through the salivary ducts. We found that plasmid DNA is uptaken: i) by all the cells of the parenchyma, when administered alone, ii) by large ducts and to a lesser extent by the acinar cells, when administered together with replication-deficient adenovirus subtype 5 (rAd5) empty particles, and iii) by acinar cells, when

compensatory endocytosis is elicited during beta-adrenergic stimulation. Finally, we showed that plasmid DNA follows different internalization routes, and regardless the modality of internalization, escapes the lysosomal degradative pathway and the retrograde pathway towards the Golgi apparatus.

Material and Methods

Animals

Sprague–Dawley male rats weighing 150 – 250 g were obtained from Harlan Laboratories Inc. (Frederick, MD). The animals were acclimated for one week before used for the procedures. Water and food were provided *ad libitum*. All the experiments were approved by the National Institute of Dental and Craniofacial Research (NIDCR, National Institute of Health, Bethesda, MD, USA) Animal Care and Use Committee.

Plasmids and adenovirus

To characterize the internalization of plasmid DNA, pVenus A206K (gift from Dr. G. Patterson, NICHD, USA) was used. Plasmid was purified using a QIAfilter Plasmid Maxi Kit (Qiagen, Valencia, CA). Rhodamine CX Label IT® Nucleic Acid Labeling Kit (Mirus, Madison, WI) was used to label pVenus according to the manufacturer's instructions. rAd5 encoding no protein (C. Goldsmith, NIDCR, USA) was prepared and purified using Vivapure Adenopack (Sartorius Stedim North America Inc., Bohemia, NY). Viral titer was determined by measuring the optical absorbance at 260 nm (Green and Pina, 1963; Green et al., 1967).

In vivo gene delivery into SMGs

For the *in vivo* gene delivery, plasmid DNA was diluted with saline at the appropriate concentration with or without viral particles. The animals were anesthetized by an intra muscular injection of a mixture of 100 mg/Kg ketamine (Fort Dodge Animal Health, Fort Dodge, IA) and 20 mg/Kg xylazine (Akorn Inc., Decatur, IL). A fine polyethylene cannula (PE5, Strategic Applications, Inc., Libertyville, IL) was inserted intraorally in the orifice of the Wharton's duct and sealed with glue (Elmer's Products Inc., Columbus, OH). The appropriate amount of plasmid DNA (100 μl/gland) was slowly injected to avoid any damage, and the cannulae were removed after 10 minutes. When needed, isoproterenol (Sigma, St. Louis, MO), an agonists of beta-adrenergic receptors, was administrated subcutaneously (0.25 mg/kg).

Administration of drugs through the Wharton's duct

20 mM Amiloride (Sigma, St. Louis, MO), 10 μm Latrunculin A (Lat A) (Sigma, St. Louis, MO) or saline, as control, were retro-injected into the Wharton's duct of anesthetized rat submandibular glands as described above (100 μl per gland). After 20 minutes, plasmid DNA encoding for pVenus was retro-injected either alone or in the presence of rAD5 particles. After 16 hrs the submandibular glands were excised and imaged by using two-photon microscopy (Excitation wavelength 930 nm). The number of cells expressing the transgene was calculated as previously described (Sramkova et al., 2009). Cells expressing the transgene were counted in a randomly selected field (area of each field 1.61 mm^2). For each gland 10 random fields were counted. For each animal, 2 glands were evaluated, and for each drug two animals were used. Data are expressed as average cell per mm^2 +/− S.D.

Immunocytochemistry

SMGs were snap frozen in liquid nitrogen using the optimum cutting temperature compound (Sakura Finetek USA Inc., Torrance, CA), cut on silanated glass slides (20 μm thickness)

and fixed for 15 min in 2% formaldehyde at R.T. Cryosections were incubated with blocking solution for 45 min followed by incubation with the appropriate primary antibody or with Alexa 488-Phalloidin (Invitrogen, Carlsbad, CA) or TRITC-Phalloidin (Sigma, St. Louis, MO). The primary antibodies used in this study were the following: rabbit anti-Lamp-1 (Novus Biologicals Inc., Littleton, CO), rabbit anti-Ki67 and mouse anti-clathrin (Abcam Inc., Cambridge, MA), mouse anti-TnfR (Zymed, Carlsbad, CA), mouse anti-caveolin (BD Biosciences, San Jose, CA), and goat anti-CAR (R&D Systems, Minneapolis, MN). Alexa conjugated secondary antibodies were from Invitrogen (Carlsbad, CA).

Confocal microscopy and two-photon microscopy

A modified IX81 inverted microscope equipped with a Fluoview 1000 scanning head (Olympus America Inc., Center Valley, PA) was used both in confocal modality as described in Masedunskas et al., 2011, or in two-photon modality as described in Masedunskas and Weigert, 2008. For intravital microscopy the salivary glands were exposed and prepared as described in Masedunskas and Weigert, 2008.

Image processing and analysis of colocalization

When needed, the background noise was reduced by applying to each image one or two rounds of a 2 × 2 pixel low-pass filter by using METAMORPH (Molecular Devices). Brightness, contrast and gamma correction were applied. Volume rendering was performed using IMARIS 5.6 and 6.0 64 bit (Bitplane). The final preparation of the images was conducted with ADOBE PHOTOSHOP CS. For the quantitative analysis of the colocalization between Rh-pVenus and either EEA1 or dextran we followed the procedure described in Bolte and Cordelieres, 2006. This method is based on the determination of the Manders' coefficient, which provides an estimate of the overlap between two fluorescent signals. For each experimental condition 10 random images were acquired from 2 animals. The images were processed with the plugs-in JACP from ImageJ (NIH) to calculate the Mander's coefficent. Automatic thresholdin was applied. Data were expressed as average +/− SD.

Proliferative index

For each animal, a salivary gland was excised and processed for immunocytochemistry as described above. Samples were labeled for Ki67, Hoechst and F-actin. Three cryo-sections were evaluated. For each cryosections a Z-stack was acquired by using confocal microscopy. The proliferative index (PI) is reported here as a percentage of Ki67-positive nuclei vs. the total nuclei.

Results and discussion

The modality of administration of plasmid DNA affects the pattern of expression of reporter molecules in the submandibular glands of live rats (Sramkova et al., 2009). Indeed, we have shown that reporter molecules are expressed: 1) in the intercalated ducts (ID), when plasmid DNA is injected alone, 2) in large ducts (granular convoluted tubules, GCT, and striated ducts, SD) and in few acinar cells (AC), when plasmid DNA is mixed with rAd5 particles, and 3) exclusively in acinar cells, when plasmid DNA is injected and compensatory endocytosis is elicited by stimulation of beta-adrenergic receptors (Fig. 1a). We reasoned that these patterns of expression could be related to differences in the internalization of plasmid DNA in the various populations of the epithelial cells forming the submandibular glands. To address this point, we labeled a plasmid DNA encoding for pVenus (a monomeric variant of the yellow fluorescent protein) with Rhodamine-CX (Rh-pVenus), which enabled imaging its localization and trafficking (see Material and Methods) (Fig. 1b). Since the conjugation of plasmid DNA affected the yield of expression of the reporter

molecule (not shown), we used a mixture of labeled and unlabeled DNA. After 16h from the injection we observed that the labeled DNA was internalized by all the cells expressing the reporter molecules (Fig. 1c, arrows). Moreover, the number of transfected cells was not affected by the labeled DNA (data not shown), making this probe suitable as a tool to study the trafficking of plasmid DNA *in vivo*.

Distribution of injected Plasmid DNA in the submandibular glands of live rats

Next, we investigated how the internalization of plasmid DNA was affected by the modality of administration. To this aim, labeled plasmid DNA was retro-injected into the Wharton's duct in the presence or in the absence of rAd5, or after the stimulation of compensatory endocytosis via subcutaneous injection (SC) of isoproterenol (ISOP), an agonist of the beta-adrenergic receptor (Masedunskas et al., 2011; Sramkova et al., 2009). After 1 hour, the glands were removed and processed for immunocytochemistry. The actin cytoskeleton was labeled to identify the various types of epithelial cells in the salivary glands, based on their morphology (Hand et al., 1987; Matsuoka et al., 2000; Sramkova et al., 2009). In the absence of rAd5, labeled DNA was found in all the cells of the parenchyma (Fig. 2a), consistent with the fact that epithelial cells in rat submandibular glands are able to constitutively internalize various molecules from the apical plasma membrane (Hand et al., 1987; Matsuoka et al., 2000). However, this pattern was not consistent with the expression of the reporter molecule that is restricted to the intercalated ducts (Sramkova et al., 2009). We reasoned that in order to achieve the expression of the transgene, plasmid DNA has to gain access to the transcription machinery in the nucleus. This can occur either if the plasmids harbor a nuclear localization signal or when the nuclear envelop breaks down during mitosis. Based on the sequence of the plasmid DNA used in this study we could rule out the former. As for the latter, previous reports suggested that intercalated ducts have a high proliferative activity (Man et al., 2001; Yagil et al., 1985). Indeed, we observed that 10% of the cells in the salivary gland epithelium are positive for Ki67, a well– established marker for cell proliferation (Fig. 2c). Since we were not successful at labeling the intercalated ducts by immunofluorescence using known markers, we identified them by morphological criteria, as previously described (Sramkova et al., 2009). Specifically, in rat submandibular glands there are two kinds of intercalated ducts: the proximal, which connect adjacent acini (Fig. 2b, arrows and blu) and the distal, which connect the proximal to the large ducts (Fig. 2b, arrowhead and yellow) (Brocco and Tamarin, 1979). We observed several Ki67 positive nuclei in both proximal (Fig. 2d-1) and distal (Fig. 2d-2) ducts. Although, this is not a direct evidence, our data are consistent with the idea that plasmid DNA may gain access to the transcription machinery during mitosis.

In the presence of rAd5, labeled DNA was observed primarily in large ducts and to a limited extent in few acinar cells (Fig. 3a), closely matching the pattern of transduction previously described (Sramkova et al., 2009). In cell cultures and in tissues, it has been shown that Ad5 binds the coxsackie and adenovirus receptor (CAR). In addition, two members of the integrin family namely, αvβ5 and αvβ3, are known to mediate its internalization via clathrin-dependent endocytosis internalization (Davis et al., 2004; Meier and Greber, 2004; Walters et al., 2001). We found that CAR localized at the apical plasma membrane of both the large ducts and some acinar cells (Fig. 3b). Moreover, we found that clathrin localized close to the apical plasma membrane both in acini and ducts (Fig. 3c) as well as β3-integrin (Fig. 3d). In our hands several antibodies against αv and β5 did not produce a consistent staining by immunofluorescence. However, αvβ5 and αvβ3 have been previously reported to be localized at the apical plasma membrane in salivary glands (Delporte et al., 1997; Webster et al., 1994). These findings may suggest that either rAd5 stimulates endocytosis in the large ducts, or that plasmid DNA binds to the viral particles and this complex is internalized via the same endocytic route utilized by the Ad5 virus. Although we have not

been able to directly test whether such a complex is formed, we found that the administration of rAd5 did not stimulate any form of endocytosis from the apical plasma membrane (data not shown). Moreover, the association with the rAd5 may provide the way for the plasmid DNA to reach the nucleus and access the transcription machinery. Indeed, the capsid of rAd5 has been shown to bind to the nuclear pore protein CAN/Nup24 and the molecular chaperone Hsc70, which has been suggested to facilitate the import of the adenovirus genome into the nucleus (Leopold and Crystal, 2007).

Finally, we observed that labeled DNA was internalized only by acinar cells when ISOP was injected subcutaneously to stimulate compensatory endocytosis (Fig. 3e). This pattern is fully consistent with the expression of the reporter molecule that under this condition is expressed primarily in acinar cells (Sramkova et al., 2009). Moreover, this observation is consistent with the fact that plasmid DNA was not detected in large ducts, where both exocytosis and compensatory endocytosis is under the control of alpha-adrenergic receptors (Peter et al., 1995).

Internalization of naked DNA in rat submandibular glands

In order to investigate the modality of internalization and the trafficking of plasmid DNA in live animals, we performed both intravital microscopy and immunocytochemistry at different times after its retro-injection into the Wharton's duct. Upon injection, plasmid DNA was retained into ducts (Fig. 4a, arrow) and acinar canaliculi (Fig. 4a, arrowhead) indicating that the ductal system was not damaged in spite of the slight pressure exerted during the injection. This was observed also in the presence of rAd5 (not shown). After 1-2 minutes, we observed vesicular structures containing plasmid DNA in close proximity to the apical plasma membrane, both in control conditions (not shown) and in the presence of rAd5 (Fig. 4b, arrowheads, Fig. 4c, and Suppl. movie 1). Although light microscopy does not allow a precise determination of the size of these vesicles we estimated that their apparent diameter is in the range of 0.5-1 μm. When plasmid DNA was administered either alone or in the presence of rAd5, we did not observe any co-localization with clathrin (Fig. 4d), co-injected dextran, a marker for fluid-phase endocytosis (Fig. 4e, left and center panels), or Caveolin1 (data not shown). To gain more information on this pathway, selected pharmacological inhibitors were retro-injected into the salivary glands before the administration of plasmid DNA. Since the quantitative analysis of the internalized plasmid DNA into the epithelial cells did not produce consistent results, we scored the number of cells expressing the reporter molecules after 16 hours from the injection. Transgene expression was sensitive to the administration of amiloride, an inhibitor of macropinocytosis (Fig. 4f). However it was not affected by Latrunculin A, an inhibitor of the actin cytoskeleton reported also to block macropinocyticosis (Fig. 4f) (Ivanov, 2008). These results suggest that under these conditions plasmid DNA may utilize a clathrin-independent pathway different from those that internalize fluid-phase markers. When compensatory endocytosis was stimulated, plasmid DNA internalized with dextran in slightly larger vesicles than those observed in control conditions or in the presence of rAd5. Consistent with this finding, no co-localization with clathrin was detected (Fig. 4d and 4e, lower panels) indicating that plasmid DNA utilizes a clathrin-independent form of compensatory endocytosis. Unfortunately, a further pharmacological characterization of this pathway was not possible to carry out, since even the injection of saline before the administration of ISOP affected the expression of the transgene.

After 5 minutes from the injection, we observed that in control conditions or in the presence of rAd5 particles, only few vesicular structures contained both plasmid DNA and dextran (Fig. d, right graph). These vesicles seemed to be derived from the fusion of two distinct populations of endosomal vesicles (Fig. 5a, arrows and Suppl. Movie 2), which did not colocalize with the early endosomal marker EEA1 (Fig. 5b, upper and middle panels, and

Fig. d, left graph)). On the other hand, upon stimulation with ISOP only a subpopulation of the internalized vesicles colocalized with EEA1 (Fig. 5b, lower panels – arrowheads, and Fig. 5d, left graph). After 1 hour (Fig. 5c) or 6 hours (data not shown) from the internalization, only a small percentage of plasmid DNA-containing vesicles were labeled with dextran in control condition or in the presence of rAd5 particles (Fig. 5c, arrows and Fig. 5d right graph), whereas in the animals injected with ISOP the overlap was almost complete (Fig. 5c, arrowheads and Fig. 5d right graph). These findings indicate that plasmid DNA can be internalized from the apical plasma membrane via non-clathrin dependent pathways. However, these pathways show different characteristics that may depend both by the modality of administration of plasmid DNA and by differences in the machinery of endocytosis among the various subpopulation of cells in the glandular epithelium.

Trafficking of naked DNA in rat submandibular glands

An important point we sought to address was to determine the fate of plasmid DNA after internalization. It has been suggested that plasmid DNA may escape from the endosomal system into the cytoplasm to avoid degradation in the lysosomes, and reach the nucleus (Wolff and Budker, 2005). To follow the trafficking of labeled DNA, the glands were fixed and processed for immunofluorescence after 1 hour (not shown) or 6 hours (Fig. 6), which is the earliest time point when transgene expression is detected (Sramkova et al., 2009). Plasmid DNA was localized in vesicular structures, which did not overlap with early endosomes, late endosomes/lysosomes, early or recycling endosomes, trans-Golgi network, Golgi apparatus, and secretory vesicles as assessed by using markers such as EEA1 (not shown), LAMP1, TfnR, Vamp4, GM130 (Fig. 6 and Suppl. Fig.1) and VAMP8 (not shown), respectively. The same analysis was carried out after 16 hrs from the injection with similar results (not shown).

Our findings show that at plasmid DNA is able to evade lysosomal degradation and the retrograde pathway toward the ER. Moreover, we did not observe any evidence for trafficking through the APPL-dependent pathway to the nucleus (data not shown) (Miaczynska et al., 2004). Further investigations are in progress in order to determine the nature of the compartment where plasmid DNA is localized and whether plasmid DNA may be released into the cytoplasm, as suggested by others (Khalil et al., 2006; Medina-Kauwe et al., 2005). However, we cannot rule out other possibilities. For example: i) a small fraction of the plasmid DNA beyond our detection limit may have escaped into the cytoplasm, ii) a fraction of the plasmid DNA is imported into the cytoplasm through pathway that does not involve endocytosis, or ii) plasmid DNA uses a novel route to gain access to the transcription machinery.

In conclusion, we have shown that the internalization and the trafficking of plasmid DNA can be studied in live animals. This study shows the benefits of transitioning from in vitro systems (i.e. cell cultures) to a more physiological model. Particularly for tissues such as the salivary glands, which are currently used as target organs for gene therapy in humans, it is fundamental to establish an experimental system that recapitulates the complex interplay among the various cell populations forming the epithelium and the stroma. In this respect, the salivary glands of live rats represent an ideal model system since they provide with the opportunity to perform intravital imaging and follow in real time the delivery, internalization, trafficking, and expression of plasmid DNA. Moreover, the accessibility of the submandibular glands through the Wharton's duct enables performing both pharmacological and genetic manipulations that may provide more information about gene delivery at a molecular level.

Supplementary Material

Refer to Web version on PubMed Central for supplementary material.

Acknowledgments

This research was supported by the Intramural Research Program of the NIH, National Institute of Dental and Craniofacial Research. We would like to thank Drs. Amornphimoltham and Porat-Shliom for critical reading of the manuscript.

References

Adriaansen J, Perez P, Goldsmith CM, Zheng C, Baum BJ. Differential sorting of human parathyroid hormone after transduction of mouse and rat salivary glands. Hum Gene Ther. 2008; 19:1021–1028. [PubMed: 18694295]

Adriaansen J, Perez P, Zheng C, Collins MT, Baum BJ. Human parathyroid hormone is secreted primarily into the bloodstream after rat parotid gland gene transfer. Hum Gene Ther. 2011; 22:84–92. [PubMed: 20977345]

Adriaansen J, Zheng C, Perez P, Baum BJ. Production and sorting of transgenic, modified human parathyroid hormone in vivo in rat salivary glands. Biochem Biophys Res Commun. 2010; 391:768–772. [PubMed: 19944067]

Al-Dosari MS, Gao X. Nonviral gene delivery: principle, limitations, and recent progress. Aaps J. 2009; 11:671–681. [PubMed: 19834816]

Anwer K, Bailey A, Sullivan SM. Targeted gene delivery: a two-pronged approach. Crit Rev Ther Drug Carrier Syst. 2000; 17:377–424. [PubMed: 10958247]

Baccaglini L, Hoque AT Shamsul, Wellner RB, Goldsmith CM, Redman RS, Sankar V, Kingman A, Barnhart KM, Wheeler CJ, Baum BJ. Cationic liposome-mediated gene transfer to rat salivary epithelial cells in vitro and in vivo. J Gene Med. 2001; 3:82–90. [PubMed: 11269339]

Baum BJ, Zheng C, Cotrim AP, Goldsmith CM, Atkinson JC, Brahim JS, Chiorini JA, Voutetakis A, Leakan RA, Van Waes C, Mitchell JB, Delporte C, Wang S, Kaminsky SM, Illei GG. Transfer of the AQP1 cDNA for the correction of radiation-induced salivary hypofunction. Biochim Biophys Acta. 2006; 1758:1071–1077. [PubMed: 16368071]

Bolte S, Cordelieres FP. A guided tour into subcellular colocalization analysis in light microscopy. J Microsc. 2006; 224(3):213–232. [PubMed: 17210054]

Bouard D, Alazard-Dany D, Cosset FL. Viral vectors: from virology to transgene expression. Br J Pharmacol. 2009; 157:153–165. [PubMed: 18776913]

Brocco SL, Tamarin A. The topography of rat submandibular gland parenchyma as observed with S.E.M. Anat Rec. 1979; 194:445–459. [PubMed: 475009]

Budker V, Budker T, Zhang G, Subbotin V, Loomis A, Wolff JA. Hypothesis: naked plasmid DNA is taken up by cells in vivo by a receptor-mediated process. J Gene Med. 2000; 2:76–88. [PubMed: 10809141]

Davis B, Nguyen J, Stoltz D, Depping D, Excoffon KJ, Zabner J. Adenovirus-mediated erythropoietin production by airway epithelia is enhanced by apical localization of the coxsackie-adenovirus receptor in vivo. Mol Ther. 2004; 10:500–506. [PubMed: 15336650]

Delporte C, Redman RS, Baum BJ. Relationship between the cellular distribution of the alpha(v)beta3/5 integrins and adenoviral infection in salivary glands. Lab Invest. 1997; 77:167–173. [PubMed: 9274859]

Edelstein ML, Abedi MR, Wixon J. Gene therapy clinical trials worldwide to 2007--an update. J Gene Med. 2007; 9:833–842. [PubMed: 17721874]

Fumoto S, Tsuchimochi M, Nishi J, Ishii H, Kodama Y, Nakashima M, Sasaki H, Nakamura J, Nishida K. Liver- and lobe-specific gene transfer following the continuous microinstillation of Plasmid DNA onto the liver surface in mice: effect of instillation speed. Biol Pharm Bull. 2009; 32:1298–1302. [PubMed: 19571403]

Gao R, Yan X, Zheng C, Goldsmith CM, Afione S, Hai B, Xu J, Zhou J, Zhang C, Chiorini JA, Baum BJ, Wang S. AAV2-mediated transfer of the human aquaporin-1 cDNA restores fluid secretion from irradiated miniature pig parotid glands. Gene Ther. 2011; 18:38–42. [PubMed: 20882054]

Goldfine ID, German MS, Tseng HC, Wang J, Bolaffi JL, Chen JW, Olson DC, Rothman SS. The endocrine secretion of human insulin and growth hormone by exocrine glands of the gastrointestinal tract. Nat Biotechnol. 1997; 15:1378–1382. [PubMed: 9415890]

Green M, Pina M. Biochemical studies on adenovirus multiplication. IV. Isolation, purification, and chemical analysis of adenovirus. Virology. 1963; 20:199–207. [PubMed: 13950097]

Green M, Pina M, Kimes RC. Biochemical studies on adenovirus multiplication. XII. Plaquing efficiencies of purified human adenoviruses. Virology. 1967; 31:562–565.

Hand AR, Coleman R, Mazariegos MR, Lustmann J, Lotti LV. Endocytosis of proteins by salivary gland duct cells. J Dent Res. 1987; 66:412–419. [PubMed: 3476565]

Honigman A, Zeira E, Ohana P, Abramovitz R, Tavor E, Bar I, Zilberman Y, Rabinovsky R, Gazit D, Joseph A, Panet A, Shai E, Palmon A, Laster M, Galun E. Imaging transgene expression in live animals. Mol Ther. 2001; 4:239–249. [PubMed: 11545615]

Ivanov AI. Pharmacological inhibition of endocytic pathways: is it specific enough to be useful? Methods Mol Biol. 2008; 440:15–33. [PubMed: 18369934]

Kawakami S. Development and application of glycosylated particulate carriers for delivery of nucleic acid medicine. Yakugaku Zasshi. 2008; 128:1743–1749. [PubMed: 19043293]

Kay MA. State-of-the-art gene-based therapies: the road ahead. Nat Rev Genet. 2011; 12:316–328. [PubMed: 21468099]

Khalil IA, Kogure K, Akita H, Harashima H. Uptake pathways and subsequent intracellular trafficking in nonviral gene delivery. Pharmacol Rev. 2006; 58:32–45. [PubMed: 16507881]

Lavigne MD, Gorecki DC. Emerging vectors and targeting methods for nonviral gene therapy. Expert Opin Emerg Drugs. 2006; 11:541–557. [PubMed: 16939390]

Lechardeur D, Lukacs GL. Intracellular barriers to non-viral gene transfer. Curr Gene Ther. 2002; 2:183–194. [PubMed: 12109215]

Leopold PL, Crystal RG. Intracellular trafficking of adenovirus: many means to many ends. Adv Drug Deliv Rev. 2007; 59:810–821. [PubMed: 17707546]

Man YG, Ball WD, Marchetti L, Hand AR. Contributions of intercalated duct cells to the normal parenchyma of submandibular glands of adult rats. Anat Rec. 2001; 263:202–214. [PubMed: 11360236]

Masedunskas, A.; Porat-Shliom, N.; Weigert, R. Regulated exocytosis: novel insights from intravital microscopy. Traffic. 2012.

Masedunskas A, Sramkova M, Parente L, Sales KU, Amornphimoltham P, Bugge TH, Weigert R. Role for the actomyosin complex in regulated exocytosis revealed by intravital microscopy. Proc Natl Acad Sci U S A. 2011; 108:13552–13557. [PubMed: 21808006]

Masedunskas A, Weigert R. Intravital two-photon microscopy for studying the uptake and trafficking of fluorescently conjugated molecules in live rodents. Traffic. 2008; 9:1801–1810. [PubMed: 18647170]

Matsuoka T, Aiyama S, Kikuchi KI, Koike K. Uptake of cationized ferritin by the epithelium of the main excretory duct of the rat submandibular gland. Anat Rec. 2000; 258:108–113. [PubMed: 10603454]

Medina-Kauwe LK, Xie J, Hamm-Alvarez S. Intracellular trafficking of nonviral vectors. Gene Ther. 2005; 12:1734–1751. [PubMed: 16079885]

Meier O, Greber UF. Adenovirus endocytosis. J Gene Med. 2004; 6(Suppl 1):S152–163. [PubMed: 14978758]

Miaczynska M, Christoforidis S, Giner A, Shevchenko A, Uttenweiler-Joseph S, Habermann B, Wilm M, Parton RG, Zerial M. APPL proteins link Rab5 to nuclear signal transduction via an endosomal compartment. Cell. 2004; 116:445–456. [PubMed: 15016378]

Niedzinski EJ, Chen YJ, Olson DC, Parker EA, Park H, Udove JA, Scollay R, McMahon BM, Bennett MJ. Enhanced systemic transgene expression after nonviral salivary gland transfection using a novel endonuclease inhibitor/DNA formulation. Gene Ther. 2003a; 10:2133–2138. [PubMed: 14625568]

Niedzinski EJ, Olson DC, Chen YJ, Udove JA, Nantz MH, Tseng HC, Bolaffi JL, Bennett MJ. Zinc enhancement of nonviral salivary gland transfection. Mol Ther. 2003b; 7:396–400. [PubMed: 12668135]

Passineau MJ, Zourelias L, Machen L, Edwards PC, Benza RL. Ultrasound-assisted non-viral gene transfer to the salivary glands. Gene Ther. 2010; 17:1318–1324. [PubMed: 20508599]

Perez P, Adriaansen J, Goldsmith CM, Zheng C, Baum BJ. Transgenic alpha-1-antitrypsin secreted into the bloodstream from salivary glands is biologically active. Oral Dis. 2011; 17:476–483. [PubMed: 21122036]

Peter B, Van Waarde MA, Vissink A, s-Gravenmade EJ, Konings AW. Degranulation of rat salivary glands following treatment with receptor-selective agonists. Clin Exp Pharmacol Physiol. 1995; 22:330–336. [PubMed: 7554423]

Samuni Y, Cawley NX, Zheng C, Cotrim AP, Loh YP, Baum BJ. Sorting behavior of a transgenic erythropoietin-growth hormone fusion protein in murine salivary glands. Hum Gene Ther. 2008; 19:279–286. [PubMed: 18303958]

Schnitzer JE, Oh P, Pinney E, Allard J. Filipin-sensitive caveolae-mediated transport in endothelium: reduced transcytosis, scavenger endocytosis, and capillary permeability of select macromolecules. J Cell Biol. 1994; 127:1217–1232. [PubMed: 7525606]

Sramkova M, Masedunskas A, Parente L, Molinolo A, Weigert R. Expression of plasmid DNA in the salivary gland epithelium: novel approaches to study dynamic cellular processes in live animals. Am J Physiol Cell Physiol. 2009; 297:C1347–1357. [PubMed: 19794147]

Varkouhi AK, Scholte M, Storm G, Haisma HJ. Endosomal escape pathways for delivery of biologicals. J Control Release. 2011; 151:220–228. [PubMed: 21078351]

Walters RW, van't Hof W, Yi SM, Schroth MK, Zabner J, Crystal RG, Welsh MJ. Apical localization of the coxsackie-adenovirus receptor by glycosyl-phosphatidylinositol modification is sufficient for adenovirus-mediated gene transfer through the apical surface of human airway epithelia. J Virol. 2001; 75:7703–7711. [PubMed: 11462042]

Walther W, Stein U. Viral vectors for gene transfer: a review of their use in the treatment of human diseases. Drugs. 2000; 60:249–271. [PubMed: 10983732]

Webster P, Vanacore L, Nairn AC, Marino CR. Subcellular localization of CFTR to endosomes in a ductal epithelium. Am J Physiol. 1994; 267:C340–348. [PubMed: 7521124]

Weigert R, Sramkova M, Parente L, Amornphimoltham P, Masedunskas A. Intravital microscopy: a novel tool to study cell biology in living animals. Histochem Cell Biol. 2010; 133:481–491. [PubMed: 20372919]

Wolff JA, Budker V. The mechanism of naked DNA uptake and expression. Adv Genet. 2005; 54:3–20. [PubMed: 16096005]

Wolff JA, Dowty ME, Jiao S, Repetto G, Berg RK, Ludtke JJ, Williams P, Slautterback DB. Expression of naked plasmids by cultured myotubes and entry of plasmids into T tubules and caveolae of mammalian skeletal muscle. J Cell Sci. 1992; 103(Pt 4):1249–1259. [PubMed: 1487500]

Wolff JA, Malone RW, Williams P, Chong W, Acsadi G, Jani A, Felgner PL. Direct gene transfer into mouse muscle in vivo. Science. 1990; 247:1465–1468. [PubMed: 1690918]

Xu J, Yan X, Gao R, Mao L, Cotrim AP, Zheng C, Zhang C, Baum BJ, Wang S. Effect of irradiation on microvascular endothelial cells of parotid glands in the miniature pig. Int J Radiat Oncol Biol Phys. 2010; 78:897–903. [PubMed: 20832188]

Yagil C, Michaeli Y, Zajicek G. Compensatory proliferative response of the rat submandibular salivary gland to unilateral extirpation. Virchows Arch B Cell Pathol Incl Mol Pathol. 1985; 49:83–91. [PubMed: 2862738]

Young LS, Searle PF, Onion D, Mautner V. Viral gene therapy strategies: from basic science to clinical application. J Pathol. 2006; 208:299–318. [PubMed: 16362990]

Zheng C, Baum B. Including the p53 ELAV-like protein-binding site in vector cassettes enhances transgene expression in rat submandibular gland. Oral Dis. 2011

Zheng C, Baum BJ. Evaluation of viral and mammalian promoters for use in gene delivery to salivary glands. Mol Ther. 2005; 12:528–536. [PubMed: 16099414]

Zheng C, Cotrim AP, Rowzee A, Swaim W, Sowers A, Mitchell JB, Baum BJ. Prevention of radiation-induced salivary hypofunction following hKGF gene delivery to murine submandibular glands. Clin Cancer Res. 2011a; 17:2842–2851. [PubMed: 21367751]

Zheng C, Goldsmith CM, Mineshiba F, Chiorini JA, Kerr A, Wenk ML, Vallant M, Irwin RD, Baum BJ. Toxicity and biodistribution of a first-generation recombinant adenoviral vector, encoding aquaporin-1, after retroductal delivery to a single rat submandibular gland. Hum Gene Ther. 2006; 17:1122–1133. [PubMed: 17069536]

Zheng C, Shinomiya T, Goldsmith CM, Di Pasquale G, Baum BJ. Convenient and reproducible in vivo gene transfer to mouse parotid glands. Oral Dis. 2011b; 17:77–82. [PubMed: 20646229]

Zheng C, Voutetakis A, Goldstein B, Afione S, Rivera VM, Clackson T, Wenk ML, Boyle M, Nyska A, Chiorini JA, Vallant M, Irwin RD, Baum BJ. Assessment of the safety and biodistribution of a regulated AAV2 gene transfer vector after delivery to murine submandibular glands. Toxicol Sci. 2011c; 123:247–255. [PubMed: 21625005]

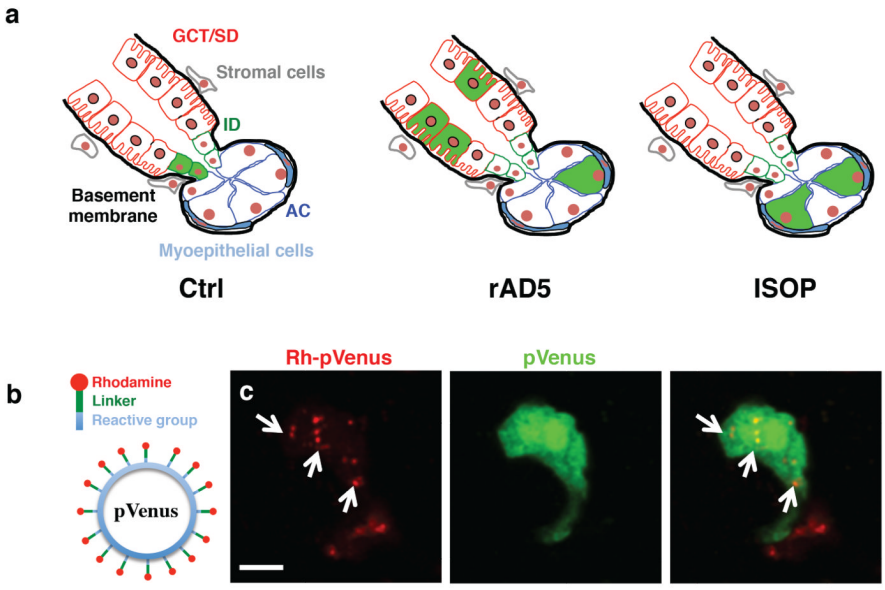

Figure 1. Expression of the transgene in rat submandibular glands after retro-injection of plasmid DNA

a) Diagram showing the pattern of transgene expression in the submandibular salivary glands of live rats after the injection of plasmid DNA alone, in the presence of empty rAD5 particles, or upon SC injection of ISOP (Sramkova et al., 2009). When plasmid DNA is injected alone, the transgene is expressed in the intercalated ducts (ID). In the presence of rAd5, the transgene is expressed in the large ducts (granular convoluted tubules (GCT) and striated ducts (SD)), and in few cells of the acini (AC). Upon SC injection of ISOP, the trasngene is expressed primarily in the AC. **b**) Plasmid DNA encoding for pVenus was cross-linked with Rhodamine-CX (Rh-pVenus) as described in Material and Methods. **c**) Six μg of plasmid DNA encoding for pVenus were mixed with 6 μg of Rh-pVenus and injected into the Wharton's ducts of anesthetized rats. After 16 hours, the glands were excised and imaged by two-photon microscopy (excitation wavelength 930 nm) using a 60x water immersion objective (NA 1.2). Rh-pVenus (red) was detected in small puncta in cells expressing pVenus (green). Bar 10 μm.

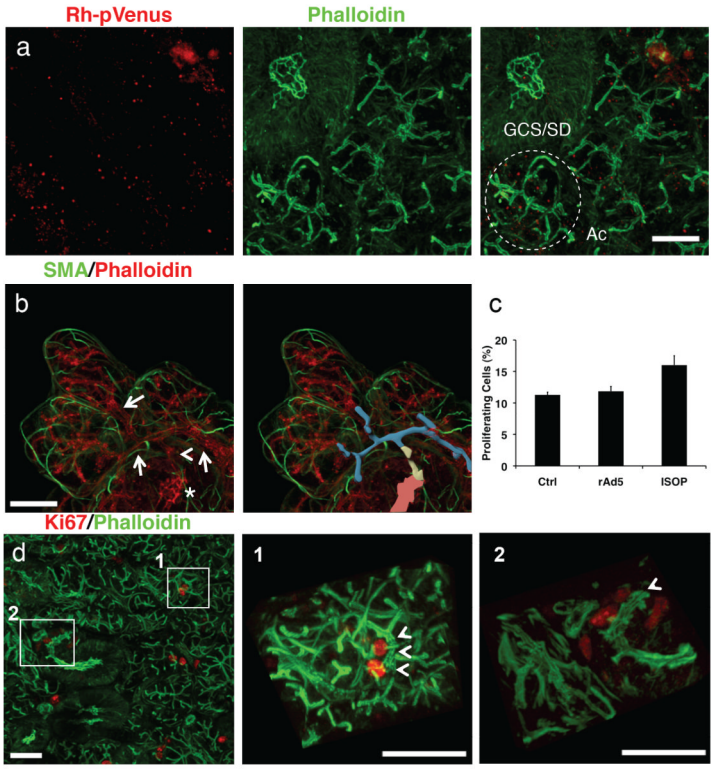

Figure 2. Plasmid DNA is internalized by all the cells in the salivary gland epithelium

a) Five μg of Rh-pVenus were retro-injected into the Wharton's duct of anesthetized rats. After 1 hour the glands were excised, processed for immunochemistry, labeled with Alexa-488 phalloidin to reveal the actin cytoskeleton (green), and imaged by confocal microscopy. Rh-pVenus (red) was distributed uniformly in the salivary glands epithelium. Bar 20 μm. **b**) Identification of the intercalated ducts. Rat submandibular salivary glands were excised and labeled with both Rhodamine-phalloidin (red) and an antibody against smooth muscle actin (SMA). A z-stack was acquired by confocal microscopy and a 3D reconstruction generate by Imaris. SMA (green) highlights the myoepithelial cells whereas actin (red) outlines the canaliculi and the ductal system. The proximal IDs connect adjacent acini have a larger diameter the canaliculi (arrows and blue outline). The distal IDs connect the proximal IDs (arrowhead and yellow outline) with the large ducts (asterisk and pink outline). Bar 20 μm. **c**) Quantification of proliferating cells in the rat submandibular glands in control conditions (Ctrl, retro-injection of saline), upon retro-injection of 3×10^{10} rAD5 particles, or after stimulation with 0.25mg/kg ISOP (see Material and Methods). **d)** Identification of proliferating cells in rat submandibular glands. Submandibular glands were excised, processed for immunofluorescence, stained with an antibody directed against anti-Ki67 (red) and Alexa488-Phalloidin (green), and imaged by confocal microscopy. Overview of a large area of the salivary glands epithelium (left panel). Proliferating cells in the proximal IDs (inset 1) and in the distal IDs (inset 2). Bars, 20 μm

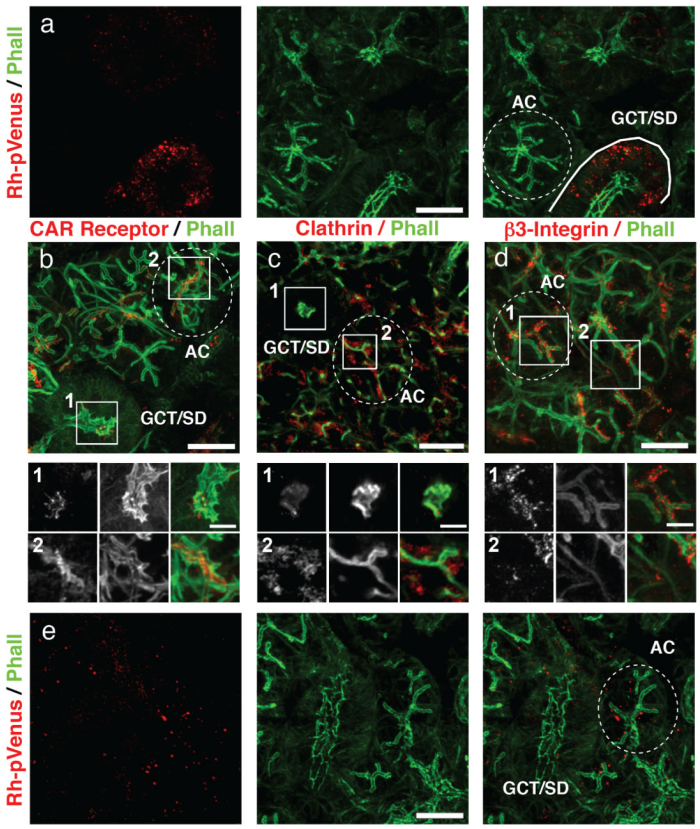

Figure 3. Plasmid DNA is internalized in large ducts in the presence of rAD5 or in acinar cells upon stimulation of compensatory endocytosis

Five μg of Rh-pVenus were retro-injected into the submandibular salivary glands of a live rat as described in legend to Fig. 2 eitherin presence of 3×10^{10} rAd5 particles (**a**) or upon SC injection of 0.25mg/kg ISOP (**d**). After 1 hour the glands were excised, processed for immunofluorescence to reveal actin (green), and imaged by confocal microscopy. **a**) Rh-pVenus (red) was internalized by GCT, SD (solid line) and to a limited extent by AC (dotted line). Bar 20 μm. **b-d**) Submandibular salivary glands were processed for immunofluorescence, stained with Alexa 488-phalloidin (green) and either an antibody against the CAR receptor (**b**, red), clathrin (**c**, red), or β3-integrin (**d**, red). Both CAR receptor (**b**) and clathrin (**c**) are localized in large ducts (**b**, inset 1 and c, inset 1) and in acini (**b**, inset 2 and c, dotted circle). β3-integrin localizes both at the apical (**d**, inset 1) and the basolateral membrane (**d**, inset 2). Bars, 20 μm. **e**) Rh-pVenus was internalized by acinar cells. Bar 20 μm.

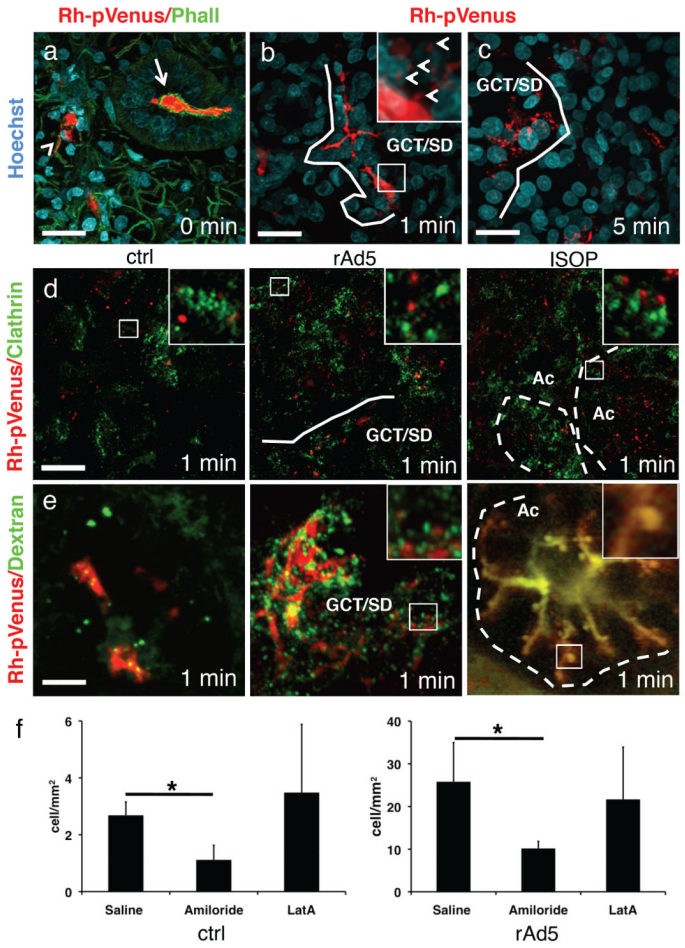

Figure 4. Internalization of plasmid DNA from the apical plasma membrane of the salivary glands epithelium

Five μg of Rh-pVenus were retro-injected into the Wharton's duct either alone (**a-d**) or mixed with 20 μg of 70 kDa Alexa 488-dextran (**e**) as described in Material and Methods. The injections were performed without any further manipulation (**a**, **d** and **e**, left panels), in the presence of 3×10^{10} rAd5 particles (**b, c**, and **d** and **e**, center panels), or upon SC injection of 0.25mg/kg ISOP (**d** and **e**, right panels). The glands were excised immediately (**a**), after 1 (**b, e**), 2 **(d)**, or 5 minutes (**c**) from the injection. Large ducts (GCT/SD) were highlighted by solid lines, whereas acini (Ac) were highlighted by dotted lines. **a-d**) The excised glands were labeled with Hoechst (cyan) and Alexa-488 phalloidin (**a**, green), or with an antibody against clathrin (**d**, green) and imaged by confocal microscopy. Initially, Rh-pVenus (red) was localized in the ducts (**a**, arrow) and after 1 min was present in vesicles budding from the ducts (**b**, solid line and inset). After 5 minutes, several vesicles containing Rh-pVenus were detected (**c**). **d**) Rh-pVenus-containing vesicles did not colocalize with clathrin under any of the experimental conditions. Bar 20 μm. **e**) Rh-pVenus (red) and Alexa 488-dextran (green) were localized in different vesicles under control conditions or in the presence of rAd5 (left and center panels), whereas they were present in the same structures upon injection of ISOP. Bar, 10 μm. **f**) Saline, 20 mM Amiloride or 10 μm Latrunculin A (Lat A) were retro-injected in the Wharton's duct of anesthetized rats. After 20 min, 12 μg of a plasmid encoding for pVenus were retro-injected either in control conditions or in the presence of 3×10^{10} rAd5 particles. After 16 hours the number of cells

expressing the transgene was determined as described in Material and Methods. Data are expressed in number of cell expressing the transgene per mm^2 +/− S.D. Statistical significance was calculated using t-test with * $p<0.05$. Data are representative of a single experiment. The experiment was repeated twice with similar results.

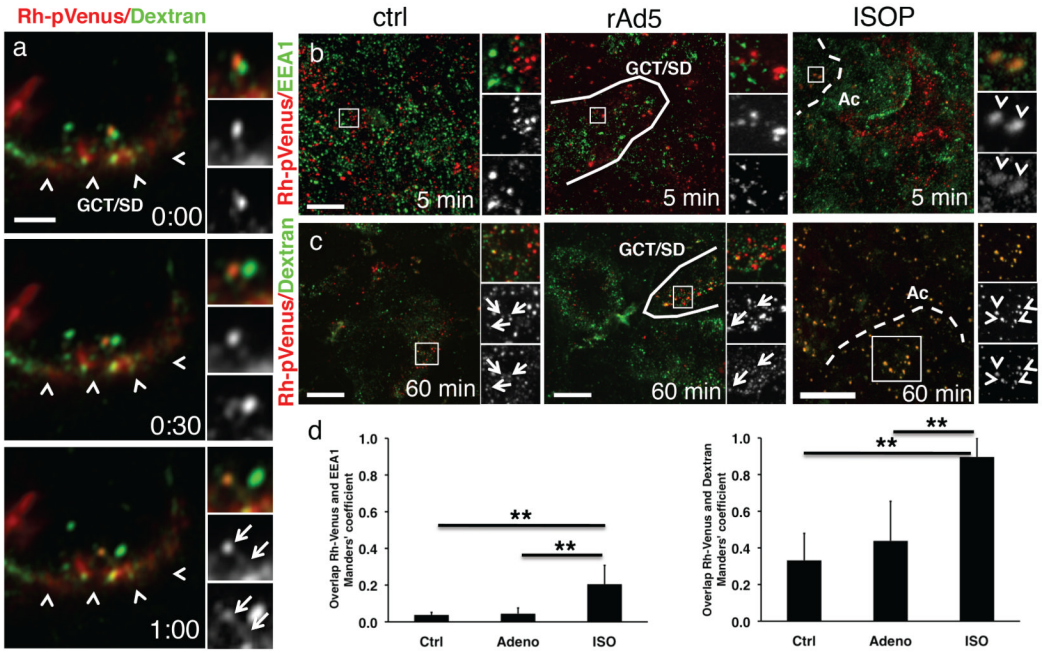

Figure 5. Plasmid DNA localizes in endosomal structures after the internalization

Five μg of Rh-pVenus were retro-injected into the Wharton's duct either alone (**b**, suppl. movie 1) or in the presence of 20 μg Alexa 488-dextran (**a,c**, suppl. movie 2). The injections were performed without any further manipulation (**b, c** upper panels), in the presence of 3×10^{10} rAd5 particles (**a**, **b** and **c**, center panels), or upon SC injection of 0.25mg/kg ISOP (**b** and **c**, lower panels). **a**) The submandibular glands of anesthetized rats were exposed and imaged by time-lapse intravital two-photon microscopy (Excitation wavelength 930 nm). Rh-pVenus- and Alexa 488-dextran-containing endosomes are internalized from a large duct (arrowheads) separately in endocytic vesicles that after few minutes fuse together (arrows). Bar 10 μm. **b**, **c**) The submandibular salivary glands were excised after either 5 (**b**) or 60 (**c**) minutes from the injection and processed for immunofluorescence. **b**) Under both control conditions and in the presence of rAd5 particles, Rh-pVenus did not colocalize with EEA1 a marker for the early endosomes. Upon injection of ISOP, only a subpopulation of endosomes Rh-pVenus (red) co-localized with EEA1 (green, and arrowheads in the inset). Bar 20 μm. **c**) Under both control conditions and in the presence of rAd5 particles, only a subpopulation of Rh-pVenus was present in vesicles containing dextran (arrows). On the other hand, upon injection of ISOP the co-localization between Rh-pVenus and dextran was almost complete. Bars, 20 μm. **d**) Quantitative analysis of the colocalization between Rh-pVenus and either EEA1 (left, graph) or dextran (right graph). Colocalization is expressed by the Manders' coefficient as described in Material and Methods. Statistical significance was calculated using t-test with ** $p<0.01$. Data are representative of a single experiment. The experiment was repeated twice with similar results.

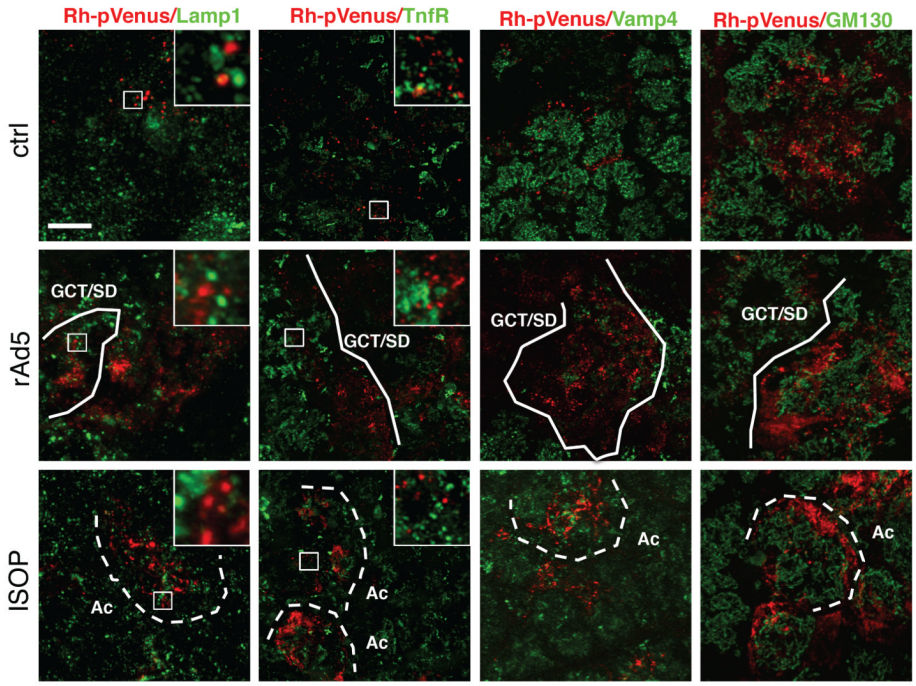

Figure 6. Plasmid DNA escapes from the both lysosomal degradation and the retrograde pathway toward the Golgi apparatus

a) Five μg of Rh-pVenus (red) were retro-injected into the Wharton's duct under the experimental conditions described in legend to Fig. 2 and 3. After 6 hours, the glands were excised, processed for immunofluorescence, probed with antibodies against LAMP-1 (lysosomes), TnfR (early and recycling endosomes), Vamp4 (Trans Golgi Network) and GM130 (Golgi), and imaged by confocal microscopy. Bar 20 μm. Large ducts (GCT/SD) were highlighted by solid lines, whereas acini (Ac) were highlighted by dotted lines. None of the markers (green) co-localized with Rh-pVenus (red). Bar 20 μm.